Available online at www.sciencedirect.com
ScienceDirect
Journal of Sound and Vibration 306 (2007) 192–202
JOURNAL OF SOUND AND VIBRATION
www.elsevier.com/locate/jsvi

Study on the radial vibration of a new type of composite piezoelectric transducer

Shuyu Lin*

Institute of Applied Acoustics, Shaanxi Normal University, Xian, Shaanxi, 710062, China

Received 8 July 2006; received in revised form 7 February 2007; accepted 13 May 2007
Available online 28 June 2007

Abstract

In this paper, a new type of composite piezoelectric ceramic transducers is studied. The transducer consists of a piezoelectric ceramic thin ring polarized in the thickness direction and a metal thin circular ring. The radial vibration of the transducer is analyzed and its radial electro-mechanical equivalent circuit is obtained. Based on the electro-mechanical equivalent circuit, the resonance and anti-resonance frequency equations are obtained. The relationship between the resonance frequency, the anti-resonance frequency, and the effective electro-mechanical coupling coefficient and the geometrical dimensions is analyzed. Some radial composite piezoelectric transducers are designed and manufactured. The resonance frequencies and anti-resonance frequencies are measured and the effective electro-mechanical coupling coefficient is calculated. It is illustrated that the measured radial resonance frequencies are in good agreement with the theoretical results from the resonance frequency equation. The finite element method is also used to find the resonance frequency and the radial displacement distribution. It is shown that the resonance and anti-resonance frequencies from the finite element method are also in good agreement with those from the analytical method in this paper.

1. Introduction

Piezoelectric ceramic transducers are widely used for emitting and receiving sound waves in the medium. There are many kinds of piezoelectric transducers that can be excited to vibrate in different vibrational modes for different practical applications. Generally speaking, the most widely used vibrational modes in ultrasonic technology are longitudinal extensional vibrational mode, radial extensional vibrational mode, torsional vibrational mode, and flexural vibrational mode [1–7]. For underwater sound and ultrasonic applications, longitudinal composite piezoelectric transducers, which are composed of a stack of piezoelectric ceramic rings sandwiched between two metal masses are widely used and they are also referred to as sandwich transducers or Langevin composite transducers. This kind of composite transducers are mainly excited to vibrate in one-dimensional longitudinal vibrational mode and the design theory has been well developed [8–14]. The advantages of the longitudinal composite piezoelectric transducers include large power capacity, high mechanical strength, low resonance frequency, and stable vibrational performances. However, the radiating

*Tel.: +86 29 85308217; fax: +86 29 85308367.
E-mail address: sxsdsxs@snnu.edu.cn

0022-460X/$ - see front matter © 2007 Elsevier Ltd. All rights reserved.
doi:10.1016/j.jsv.2007.05.024

area of a longitudinal composite piezoelectric transducer is limited to less than a quarter wavelength because one-dimensional design theory is assumed and this requires that the lateral geometrical dimension of a longitudinal composite transducer must be much less than its longitudinal dimension.

In order to increase the radiating area of the longitudinal composite piezoelectric transducer, piezoelectric ceramic ring or tube transducers in radial vibration can be used. For the radial transducers, the sound radiation is in X–Y plane and is two-dimensional, and the radiation area is increased compared with one-dimensional longitudinal composite transducer. However, for simple radial piezoelectric ceramic transducers, which are either a piezoelectric ceramic ring or a tube, its power capacity is limited because of the fact that the mechanical strength of pure piezoelectric materials is low. To overcome this problem, the radial composite piezoelectric transducer is proposed in this paper which is similar to the longitudinal composite sandwich transducer in structure. The radial composite piezoelectric transducer is composed of a piezoelectric ceramic ring or tube and an outer metal ring or tube. It can be used as a two-dimensional high power radiator in ultrasonic technology and underwater sound. It is also expected that this kind of radial composite transducers can also be used as radial actuators and sensors in some related fields.

On the other hand, in underwater acoustics and some other fields, some new flextensional vibrational mode transducers named as moonie and cymbal transducers are developed [15–19]. They have the advantages of small volume and large vibrational displacement amplitude. In moonie or cymbal transducers, a piezoelectric ceramic thin disk polarized in its thickness direction in radial vibration is sandwiched between two metal caps which can take different shapes. The radial vibration of the piezoelectric disk is converted into the flexural vibration of the metal caps, and the metal caps in flexural vibration radiate sound wave into the surrounding medium, such as water or air. In the traditional moonie or cymbal transducers, the piezoelectric ceramic disk and the metal caps are glued together by some kind of cement. Since the cementing strength is limited, the traditional moonie or cymbal transducers cannot be excited to vibrate at a very large power level. In order to increase the power capacity of the moonie or cymbal transducers, the radial composite piezoelectric transducer can be used instead of a piezoelectric ceramic disk. In this case, the metal caps and the radial composite piezoelectric transducer can be connected together by using metal bolts, the mechanical strength is increased, and therefore the power capacity of the moonie or cymbal can be increased accordingly.

As stated above, the radial composite piezoelectric transducers can be used in ultrasonic technology, underwater sound and mechanical actuating and sensing fields. However, for the radial composite piezoelectric transducer, there is no developed design theory. In this paper, the radial composite piezoelectric transducer consisting of a piezoelectric ceramic thin ring and a metal thin circular ring is studied, its electromechanical equivalent circuit is obtained, the resonance frequency equation is derived, and its vibrational characteristics are analyzed.

2. Analysis on the radial vibration of a composite piezoelectric transducer

The radial composite piezoelectric transducer is shown in Fig. 1. In the figure, the external exciting electric field E_3 is in the thickness direction. The inner and outer radiuses of the piezoelectric ceramic ring are R_1 and R_2; the inner and outer radiuses of the metal thin ring are R_2 and R_3. The thickness of the composite transducer is h.

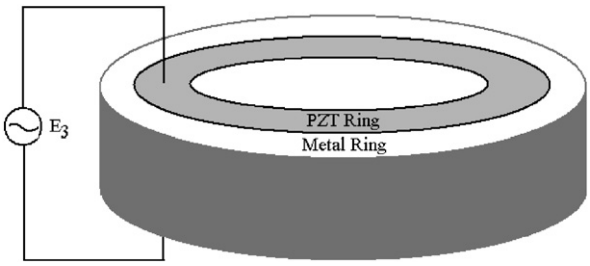

Fig. 1. Geometrical diagram of a radial composite piezoelectric transducer in radial vibration.

2.1. Radial vibration of a piezoelectric ceramic thin ring

Fig. 2 shows a thickness polarized piezoelectric ceramic ring in plane radial vibration. Its thickness, inner and outer radiuses are h, R_1, and R_2. F_{r1}, v_{r1} and F_{r2}, v_{r2} are the radial force and vibration velocity at the inner and outer surfaces of the piezoelectric ring. When the thickness is much less than the outer radius, the piezoelectric ceramic ring can be regarded as an ideal thin one and its vibration an ideal plane radial vibration. The radial wave equation is

$$\rho_0 \frac{\partial^2 \xi_r}{\partial t^2} = \frac{\partial T_r}{\partial r} + \frac{T_r - T_\theta}{r}. \tag{1}$$

Here, ρ_0 is the volume density of the piezoelectric ceramic material, r the radial coordinate, $\xi_r = \xi_r(r, t)$ the radial displacement, and T_r and T_θ the radial and tangential stresses. The radial and tangential strains S_r and S_θ can be expressed as

$$S_r = \frac{\partial \xi_r}{\partial r}, \quad S_\theta = \frac{\xi_r}{r}. \tag{2}$$

The piezoelectric constitutive equations are:

$$S_r = s_{11}^E T_r + s_{12}^E T_\theta + d_{31} E_3, \tag{3}$$

$$S_\theta = s_{12}^E T_r + s_{11}^E T_\theta + d_{31} E_3, \tag{4}$$

$$D_3 = d_{31} T_r + d_{31} T_\theta + \varepsilon_{33}^T E_3. \tag{5}$$

In the above equations, s_{11}^E and s_{12}^E are the elastic compliance constants measured at constant electric field, d_{31} the piezoelectric strain constant, E_3 the external exciting electric field, D_3 the electric displacement, and ε_{33}^T the dielectric constant measured at constant stress. Let $\xi_r = \xi_{r0}(r) \exp(j\omega t)$, using the above equations, the wave equation can be expressed as

$$d^2\xi_{r0}/dr^2 + (d\xi_{r0}/dr)/r - \xi_{r0}/r^2 + k_{r0}^2 \xi_{r0} = 0. \tag{6}$$

Here, $k_{r0} = \omega/V_{r0}$, $\omega = 2\pi f$, $V_{r0} = [1/s_{11}^E \rho_0 (1 - v_{12}^2)]^{1/2}$, V_{r0} is the radial sound speed, and $v_{12} = -s_{12}^E/s_{11}^E$. The solution to Eq. (6) is

$$\xi_{r0}(r) = A_0 J_1(k_{r0} r) + B_0 Y_1(k_{r0} r). \tag{7}$$

Here, $J_1(k_{r0}r)$ and $Y_1(k_{r0}r)$ are Bessel functions of order one, A_0 and B_0 are constants. The radial vibrational velocity amplitude v_{r0} can be obtained as

$$v_{r0} = j\omega[A_0 J_1(k_{r0} r) + B_0 Y_1(k_{r0} r)]. \tag{8}$$

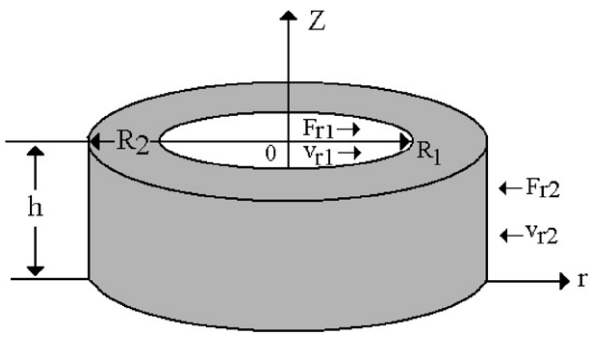

Fig. 2. A thickness polarized piezoelectric ceramic ring in radial vibration.

From Fig. 2, using the boundary conditions, $v_{r0}|_{r=R_1} = v_{r1}$, $v_{r0}|_{r=R_2} = -v_{r2}$, we can get the expressions for the constants:

$$A_0 = -\frac{1}{\mathrm{j}\omega}\frac{v_{r2}Y_1(k_{r0}R_1) + v_{r1}Y_1(k_{r0}R_2)}{J_1(k_{r0}R_2)Y_1(k_{r0}R_1) - J_1(k_{r0}R_1)Y_1(k_{r0}R_2)}, \tag{9}$$

$$B_0 = \frac{1}{\mathrm{j}\omega}\frac{v_{r2}J_1(k_{r0}R_1) + v_{r1}J_1(k_{r0}R_2)}{J_1(k_{r0}R_2)Y_1(k_{r0}R_1) - J_1(k_{r0}R_1)Y_1(k_{r0}R_2)}. \tag{10}$$

From Eqs. (3) and (4), the radial stress T_r in the piezoelectric ring can be expressed as

$$T_r = \left(\frac{S_r - S_\theta}{s_{11}^E - s_{12}^E} + \frac{S_r + S_\theta - 2d_{31}E_3}{s_{11}^E + s_{12}^E}\right)/2 = \frac{1}{s_{11}^E}\left[\frac{S_r + v_{12}S_\theta}{1 - v_{12}^2} - \frac{d_{31}E_3}{1 - v_{12}}\right]. \tag{11}$$

Substituting Eqs. (2) and (7) into (11) yields

$$\begin{aligned} T_r = {} & v_{r2}\frac{J_1(k_{r0}R_1)[k_{r0}Y_0(k_{r0}r) - Y_1(k_{r0}r)(1 - v_{12})/r] - Y_1(k_{r0}R_1)[k_{r0}J_0(k_{r0}r) - J_1(k_{r0}r)(1 - v_{12})/r]}{\mathrm{j}\omega[J_1(k_{r0}R_2)Y_1(k_{r0}R_1) - J_1(k_{r0}R_1)Y_1(k_{r0}R_2)]s_{11}^E(1 - v_{12}^2)} \\ & + v_{r1}\frac{J_1(k_{r0}R_2)[k_{r0}Y_0(k_{r0}r) - Y_1(k_{r0}r)(1 - v_{12})/r] - Y_1(k_{r0}R_2)[k_{r0}J_0(k_{r0}r) - J_1(k_{r0}r)(1 - v_{12})/r]}{\mathrm{j}\omega[J_1(k_{r0}R_2)Y_1(k_{r0}R_1) - J_1(k_{r0}R_1)Y_1(k_{r0}R_2)]s_{11}^E(1 - v_{12}^2)} \\ & - \frac{d_{31}E_3}{s_{11}^E + s_{12}^E}. \end{aligned} \tag{12}$$

From Fig. 2, we have, $F_{r1} = -T_r|_{r=R_1}S_1$, $F_{r2} = -T_r|_{r=R_2}S_2$, $S_1 = 2\pi R_1 h$, $S_2 = 2\pi R_2 h$. S_1 and S_2 are the inner and outer surface areas of the piezoelectric ceramic thin ring. Using Eq. (12) and the boundary conditions of radial forces, after some complex transformations, we have

$$F_{r1}'' = (Z_{1p} + Z_{3p})v_{r1}' + Z_{3p}v_{r2}' + N_{31}V_3, \tag{13}$$

$$F_{r2}'' = (Z_{2p} + Z_{3p})v_{r2}' + Z_{3p}v_{r1}' + N_{31}V_3. \tag{14}$$

Here, $F_{r1}'' = (\pi k_{r0}R_2/2)F_{r1}$, $F_{r2}'' = (\pi k_{r0}R_1/2)F_{r2}$, $v_{r1}' = (2/\pi k_{r0}R_2)v_{r1}$,$v_{r2}' = (2/\pi k_{r0}R_1)v_{r2}$; $N_{31} = \pi^2 k_{r0}R_1R_2(d_{31}/(s_{11}^E + s_{12}^E))$, N_{31} is the electro-mechanical conversion coefficient of a thin piezoelectric ceramic ring in radial vibration. $V_3 = E_3 h$, V_3 is the voltage applied to the piezoelectric ring. Z_{1p}, Z_{2p}, Z_{3p} are three mechanical impedances, their expressions are:

$$\begin{aligned} Z_{1p} = {} & \frac{\pi^2(k_{r0}R_2)^2 Z_{01}}{4\mathrm{j}}\left[\frac{Y_1(k_{r0}R_2)J_0(k_{r0}R_1) - J_1(k_{r0}R_2)Y_0(k_{r0}R_1)}{J_1(k_{r0}R_2)Y_1(k_{r0}R_1) - J_1(k_{r0}R_1)Y_1(k_{r0}R_2)} + \frac{1 - v_{12}}{k_{r0}R_1}\right] \\ & - \mathrm{j}\frac{Z_{01}}{2}\frac{\pi k_{r0}R_2}{J_1(k_{r0}R_2)Y_1(k_{r0}R_1) - J_1(k_{r0}R_1)Y_1(k_{r0}R_2)}, \end{aligned} \tag{15}$$

$$\begin{aligned} Z_{2p} = {} & \frac{\pi^2(k_{r0}R_1)^2 Z_{02}}{4\mathrm{j}}\left[\frac{Y_1(k_{r0}R_1)J_0(k_{r0}R_2) - J_1(k_{r0}R_1)Y_0(k_{r0}R_2)}{J_1(k_{r0}R_2)Y_1(k_{r0}R_1) - J_1(k_{r0}R_1)Y_1(k_{r0}R_2)} - \frac{1 - v_{12}}{k_{r0}R_2}\right] \\ & - \mathrm{j}\frac{Z_{02}}{2}\frac{\pi k_{r0}R_1}{J_1(k_{r0}R_2)Y_1(k_{r0}R_1) - J_1(k_{r0}R_1)Y_1(k_{r0}R_2)}, \end{aligned} \tag{16}$$

$$\begin{aligned} Z_{3p} = {} & \mathrm{j}\frac{Z_{01}}{2}\frac{\pi k_{r0}R_2}{J_1(k_{r0}R_2)Y_1(k_{r0}R_1) - J_1(k_{r0}R_1)Y_1(k_{r0}R_2)} \\ = {} & \mathrm{j}\frac{Z_{02}}{2}\frac{\pi k_{r0}R_1}{J_1(k_{r0}R_2)Y_1(k_{r0}R_1) - J_1(k_{r0}R_1)Y_1(k_{r0}R_2)}. \end{aligned} \tag{17}$$

Here, $Z_{01} = \rho_0 V_{r0} S_1$, $Z_{02} = \rho_0 V_{r0} S_2$. Let the electric current into the piezoelectric ceramic ring be I_3, For harmonic vibration, $I_3 = \mathrm{d}Q/\mathrm{d}t = \mathrm{j}\omega Q$, Q is the electrical charge. It can be calculated from the following formula:

$$Q = 2\pi \int D_3 r \, \mathrm{d}r. \tag{18}$$

Substituting Eq. (5) into Eq. (18), after some transformations, we can get the following equation:

$$I_3 = \mathrm{j}\omega C_{0r} V_3 - N_{31}(v'_{r1} + v'_{r2}). \tag{19}$$

Here, $C_{0r} = (\varepsilon_{33}^T S/h)[1 - 2d_{31}^2/(\varepsilon_{33}^T(s_{11}^E + s_{12}^E))]$, C_{0r} is the clamped electric capacitance of the piezoelectric ceramic thin ring in radial vibration. $S = \pi(R_2^2 - R_1^2)$, S is the cross-sectional area of the piezoelectric ceramic circular ring. Using Eqs. (13), (14) and (19), the Mason electro-mechanical equivalent circuit of a piezoelectric ceramic thin circular ring in radial vibration can be obtained as shown in Fig. 3. In the figure, $F''_{r1} = n_1 F_{r1}$, $F''_{r2} = n_2 F_{r2}$, $v'_{r1} = v_{r1}/n_1$, $v'_{r2} = v_{r2}/n_2$, $n_1 = \pi k_{r0} R_2/2$, $n_2 = \pi k_{r0} R_1/2$.

2.2. Plane radial vibration of a metal thin circular ring

Fig. 4 shows a metal thin circular ring in radial vibration. Its thickness, inner and outer radiuses are h, R_2, and R_3. F_{r2}, v_{r2} and F_{r3}, v_{r3} are the radial force and vibration velocity at the inner and outer surfaces of the metal ring. According to this similar type of analysis, the electro-mechanical equivalent circuit of a metal thin circular ring in radial vibration can be obtained as shown in Fig. 5. In Fig. 5, Z_{1m}, Z_{2m}, and Z_{3m} are the three mechanical impedances, their expressions are:

$$\begin{aligned} Z_{1m} = {} & \mathrm{j}\frac{2Z_{r2}}{\pi k R_2[J_1(kR_3)Y_1(kR_2) - J_1(kR_2)Y_1(kR_3)]} \\ & \times \left[\frac{J_1(kR_3)Y_0(kR_2) - J_0(kR_2)Y_1(kR_3) - J_1(kR_2)Y_0(kR_2) + J_0(kR_2)Y_1(kR_2)}{J_1(kR_2)Y_0(kR_2) - J_0(kR_2)Y_1(kR_2)}\right] \\ & - \mathrm{j}\frac{2Z_{r2}(1-\nu)}{\pi(kR_2)^2[J_1(kR_2)Y_0(kR_2) - J_0(kR_2)Y_1(kR_2)]}, \end{aligned} \tag{20}$$

$$\begin{aligned} Z_{2m} = {} & \mathrm{j}\frac{2Z_{r2}}{\pi k R_2[J_1(kR_3)Y_1(kR_2) - J_1(kR_2)Y_1(kR_3)]} \\ & \times \left[\frac{J_1(kR_2)Y_0(kR_3) - J_0(kR_3)Y_1(kR_2) - J_1(kR_3)Y_0(kR_3) + J_0(kR_3)Y_1(kR_3)}{J_1(kR_3)Y_0(kR_3) - J_0(kR_3)Y_1(kR_3)}\right] \\ & + \mathrm{j}\frac{2Z_{r3}(1-\nu)}{\pi(kR_3)^2[J_1(kR_3)Y_0(kR_3) - J_0(kR_3)Y_1(kR_3)]}, \end{aligned} \tag{21}$$

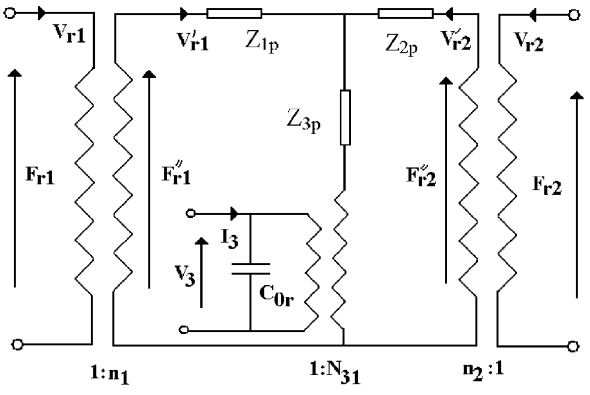

Fig. 3. Electro-mechanical equivalent circuit of a thickness polarized piezoelectric ceramic thin ring in radial vibration.

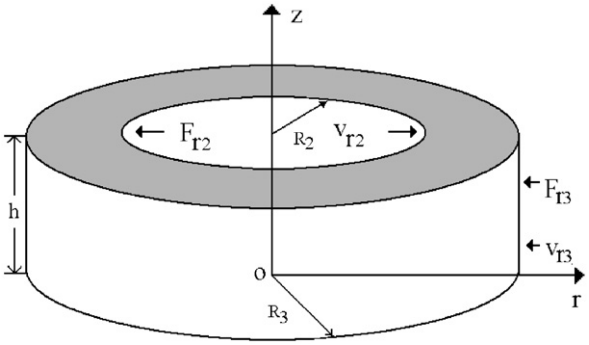

Fig. 4. A thin metal circular ring in radial vibration.

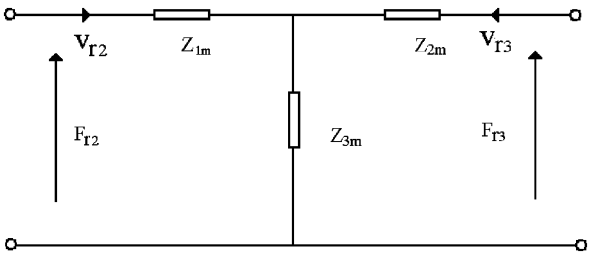

Fig. 5. Electro-mechanical equivalent circuit of a metal thin circular ring in radial vibration.

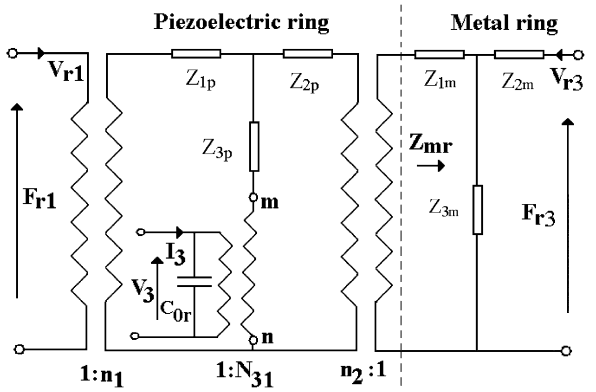

Fig. 6. Composite electro-mechanical equivalent circuit of a radial composite piezoelectric ceramic transducer in radial vibration.

$$Z_{3m} = \mathrm{j}\frac{2Z_{r2}}{\pi kR_2[J_1(kR_3)Y_1(kR_2) - J_1(kR_2)Y_1(kR_3)]} = \mathrm{j}\frac{2Z_{r3}}{\pi kR_3[J_1(kR_3)Y_1(kR_2) - J_1(kR_2)Y_1(kR_3)]}. \quad (22)$$

Here, $Z_{r2} = \rho V_r S_2$, $Z_{r3} = \rho V_r S_3$, $S_2 = 2\pi R_2 h$, $S_3 = 2\pi R_3 h$, and S_3 and S_2 are the outer and inner surface areas of the metal thin ring.

2.3. Composite electro-mechanical equivalent circuit and resonance frequency analysis of the radial composite piezoelectric ceramic transducer

At the boundary between the piezoelectric ceramic ring and the metal ring, the radial velocity and force are continuous. Using the equivalent circuits as shown in Figs. 3 and 5 derived in the above sections for the

piezoelectric ceramic ring and the metal ring, the composite electro-mechanical equivalent circuit of the radial composite piezoelectric ceramic transducer can be obtained as shown in Fig. 6. In the figure, the dotted line divides the whole figure into two parts, one representing the piezoelectric ceramic ring, and the other representing the metal ring in radial vibration.

In Fig. 6, there are two electric terminals and four mechanical terminals. When there are no external forces acting on the inner and outer surface, i.e., $F_{r1} = 0$, and $F_{r3} = 0$, the mechanical terminals of the radial transducer are short-circuited. In this case, from Fig. 6, the input mechanical impedance Z_{mr} of the metal thin circular ring in radial vibration, or the output mechanical impedance of the piezoelectric ceramic thin ring can be obtained as

$$Z_{mr} = Z_{1m} + \frac{Z_{2m}Z_{3m}}{Z_{2m} + Z_{3m}}. \tag{23}$$

The mechanical impedance Z_m between the mechanical terminals m and n of the radial composite piezoelectric ceramic transducer in radial vibration is

$$Z_m = Z_{3p} + \frac{Z_{1p}(Z_{2p} + n_2^2 Z_{mr})}{Z_{1p} + Z_{2p} + n_2^2 Z_{mr}}. \tag{24}$$

The input electric impedance Z_e of the radial composite piezoelectric ceramic transducer is

$$Z_e = \frac{V_3}{I_3} = \frac{Z_m}{N_{31}^2 + \mathrm{j}\omega C_{0r} Z_m}. \tag{25}$$

From Eq. (25), we can get the resonance frequency equation:

$$Z_e = 0. \tag{26}$$

The anti-resonance frequency equation is

$$Z_e = \infty. \tag{27}$$

Using the resonance frequency Eq. (26) and the anti-resonance frequency Eq. (27), when the material parameters and geometrical dimensions are given, the resonance frequency and the anti-resonance frequency can be calculated. On the other hand, when the resonance frequency of the transducer is given, the geometrical dimensions can also be obtained.

From the above analysis it can be seen that the frequency Eqs. (26) and (27) are complex transcendental equations, their analytical solutions are impossible to find. Therefore, numerical methods should be used. Let $R_2 = R_1 + (R_3 - R_1)\tau$, τ is known as the radius ratio. The theoretical relationship between the resonance frequency, the anti-resonance frequency, and the geometrical dimensions are computed by using the mathematical software Mathematica. The materials of the piezoelectric ceramic ring and the metal ring are PZT-4 and steel. Their standard material parameters are used and listed as follows: $\rho_0 = 7500\,\mathrm{kg/m^3}$, $s_{11}^E = 12.3 \times 10^{-12}\,\mathrm{m^2/N}$, $s_{12}^E = -4.05 \times 10^{-12}\,\mathrm{m^2/N}$, $v_{12} = 0.33$, $d_{31} = -123 \times 10^{-12}\,\mathrm{C/N}$, $\varepsilon_{33}^T/\varepsilon_0 = 1300$, $\varepsilon_0 = 8.842 \times 10^{-12}\,\mathrm{C^2/(N\,m^2)}$, $\rho = 7800\,\mathrm{kg/m^3}$, $E = 2.09 \times 10^{11}\,\mathrm{N/m^2}$, and $v = 0.28$. The theoretical relationship between the resonance frequency and radius ratio is shown in Figs. 7 and 8.

It can be seen from Figs. 7 and 8 that when radius ratio τ is increased, the first and the second resonance and anti-resonance frequency are all decreased. This means that the geometrical dimensions of the radial composite piezoelectric transducer affect its resonance and anti-resonance frequency. When the inner and outer radiuses R_1 and R_3 of the transducer are fixed, the resonance and anti-resonance frequency are decreased when the radius R_2 is increased. This means that the resonance frequency of a metal ring is higher than that of a piezoelectric ceramic ring with the same geometrical dimensions. Fig. 9 illustrates the effective electro-mechanical coupling coefficient k_{eff} of the radial composite piezoelectric transducer, its expression is

$$k_{\mathrm{eff}}^2 = \frac{f_p^2 - f_s^2}{f_p^2}. \tag{28}$$

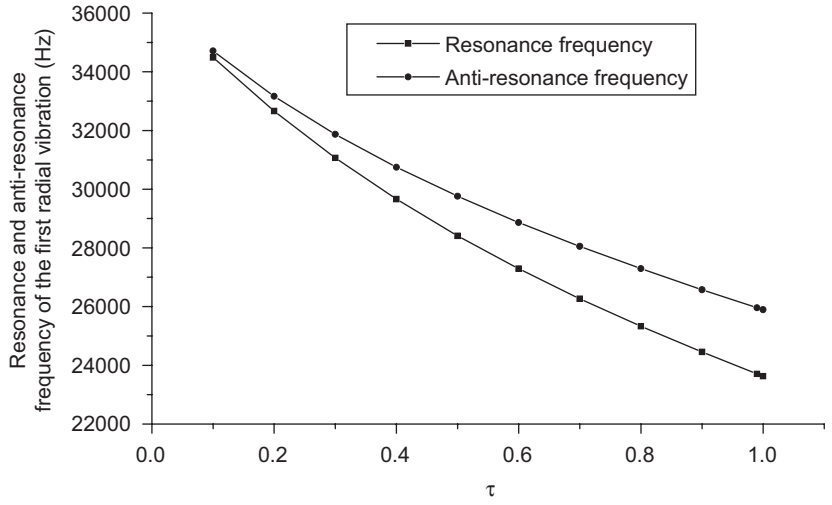

Fig. 7. Theoretical relationship between the first resonance and anti-resonance frequency and radius ratio τ.

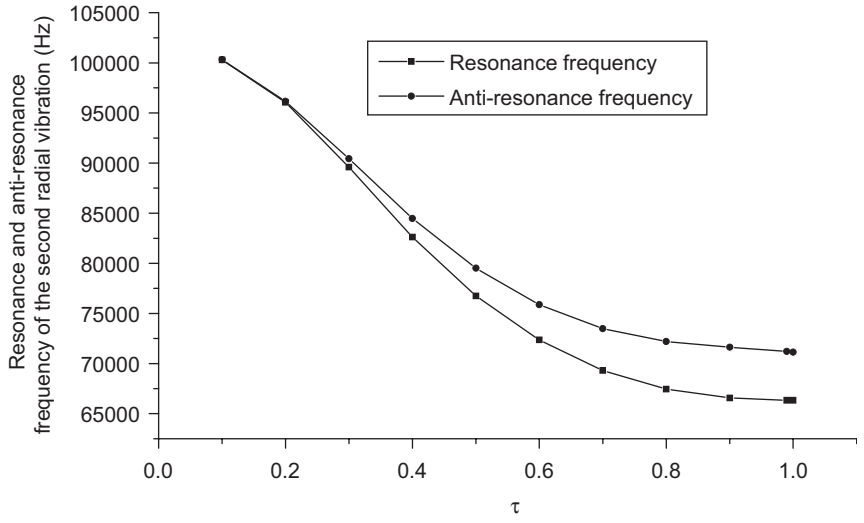

Fig. 8. Theoretical relationship between the second resonance and anti-resonance frequency and radius ratio τ.

It is shown in Fig. 9 that the effective electro-mechanical coupling coefficient is increased when the radius ratio τ is increased. The reason for this is that when the proportion of the piezoelectric ceramic material in the composite transducer is increased, the electro-mechanical conversion capacity is increased.

It is well-known that the finite element method is very useful in finding the resonance frequency and analyzing the vibrational displacement distribution of transducers with any geometrical shapes and dimensions. Table 1 illustrates the theoretical resonance frequencies of some radial composite piezoelectric transducers by using the analytical method from the resonance frequency equation and the finite element method. In Table 1, f_r and f_a are the first radial resonance and anti-resonance frequency of the transducers obtained from the frequency equations; f_{rn} and f_{an} are the first radial resonance and anti-resonance frequency of the transducers obtained from the finite element method (ANSYS Program). $\Delta 1 = |f_r - f_{\mathrm{rn}}|/f_{\mathrm{rn}}$, $\Delta 2 = |f_a - f_{\mathrm{an}}|/f_{\mathrm{an}}$. It can be seen from Table 1 that the resonance frequencies from the frequency equations and the finite element method are in good agreement with each other.

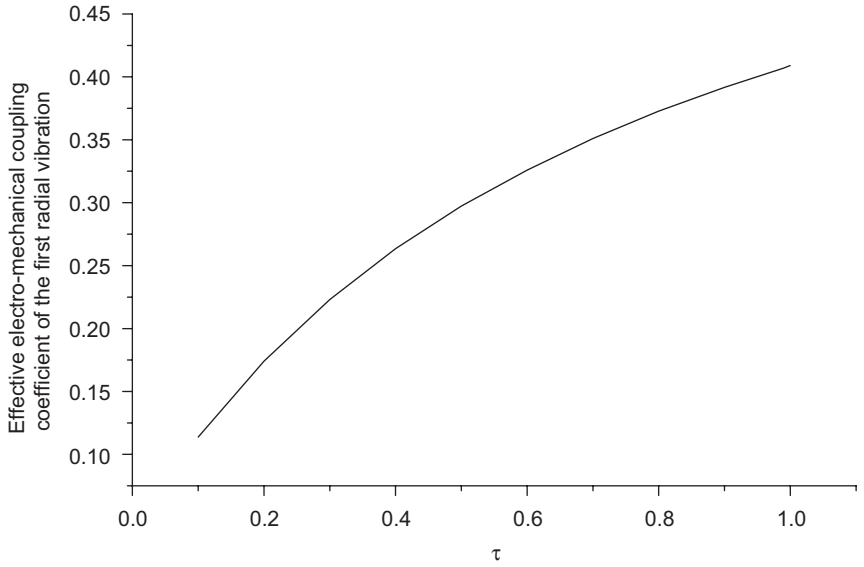

Fig. 9. Theoretical relationship between the effective electro-mechanical coupling coefficient and radius ratio τ.

Table 1
Theoretical resonance and anti-resonance frequencies of the radial composite piezoelectric transducers from the frequency equations and the finite element method

No.	R_1 (mm)	R_2 (mm)	R_3 (mm)	h (mm)	f_r (Hz)	f_a (Hz)	f_{rn} (Hz)	f_{an} (Hz)	$\Delta 1$ (%)	$\Delta 2$ (%)
1	7	26	46	6	27 781	29 638	27 740	29 768	0.15	0.44
2	6	30	50	8	25 798	27 970	25 741	28 078	0.22	0.38
3	8	20	40	6	31 761	33 066	31 726	33 097	0.11	0.09
4	4	12.5	42.5	6	36 368	37 409	36 337	37 379	0.09	0.08

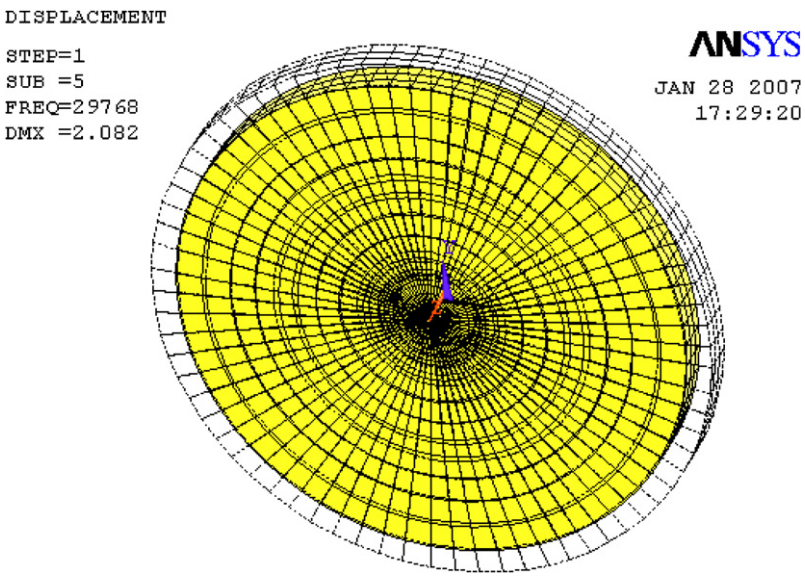

Fig. 10. The simulated vibrational displacement distribution pattern from the finite element method.

Table 2
Theoretical and measured resonance and anti-resonance frequency of the radial composite piezoelectric transducers

No.	R_1 (mm)	R_2 (mm)	R_3 (mm)	h (mm)	f_r (Hz)	f_a (Hz)	f_{rm} (Hz)	f_{am} (Hz)	$\Delta 3$ (%)	$\Delta 4$ (%)
1	7	26	46	6	27 781	29 638	28 301	29 301	1.84	1.15
2	6	30	50	8	25 798	27 970	26 476	27 167	2.56	2.96
3	8	20	40	6	31 761	33 066	32 234	32 709	1.47	1.09
4	4	12.5	42.5	6	36 368	37 409	35 917	36 335	1.26	2.96

The radial vibrational displacement distribution pattern of a radial composite piezoelectric transducer from the finite element method is simulated and shown in Fig. 10. It is obvious that the simulated vibrational distribution of the radial composite piezoelectric transducer is in the radial direction, and this is in full consistency with the analytically predicted result.

3. Experiments

In order to verify the theoretical analysis, some radial composite piezoelectric ceramic transducers are designed according to the frequency equations and manufactured. The materials of the piezoelectric ceramic ring and the metal ring are PZT-4 and steel. Their material parameters are the same as those used in the computation of the above analysis. The resonance and anti-resonance frequencies of the radial composite piezoelectric transducers are measured using an Agilent 4294A precision impedance analyzer; the measured results are listed in Table 2. In the table, f_r and f_a are the theoretical radial resonance frequency and anti-resonance frequency of the radial composite transducer from the frequency equations; f_{rm} and f_{am} are the measured resonance and anti-resonance frequency of the radial composite transducer, $\Delta 3 = |f_r - f_{rm}|/f_{rm}$, $\Delta 4 = |f_a - f_{am}|/f_{am}$. It can be seen that the measured radial resonance frequencies are also in good agreement with the theoretical results from the frequency equations.

4. Conclusions

In this paper, the radial composite piezoelectric transducer is proposed and analyzed, its radial vibration is studied analytically, and the finite element method is also used to analyze its electro-mechanical vibrational characteristics. To sum up the above analysis, the following conclusions can be obtained:

1. The electro-mechanical equivalent circuit of the radial composite piezoelectric ceramic transducer is obtained, and the resonance and anti-resonance frequency equations are derived.
2. The relationship between the resonance frequency and radius ratio of the radial composite piezoelectric transducer is analyzed. When radius ratio τ is increased, the resonance and anti-resonance frequency are decreased.
3. When the radius ratio τ is increased, the effective electro-mechanical coupling coefficient is increased.
4. The finite element method is used to find the resonance frequency and simulate the radial vibrational displacement distribution of the radial composite piezoelectric transducer. It is shown that the resonance frequencies from the frequency equations and the finite element method are in good agreement with each other.
5. Some radial composite piezoelectric transducers are designed and manufactured; the resonance and anti-resonance frequencies are measured. It is shown that the measured resonance frequencies are in good agreement with the theoretical results.
6. In this paper, it is assumed that the thickness of the transducer is much less than its outer radius. This means that the ideal plane radial vibration is assumed. The analysis for the radial composite piezoelectric transducer consisting of a piezoelectric long tube will be studied in future research work.
7. This kind of radial composite piezoelectric ceramic transducers can be as ultrasonic and underwater sound radiators with large radiation area and power. It can also be used as actuators and sensors in ultrasonic motor and other related fields.

Acknowledgments

The National Natural Science Foundation of China is acknowledged for its financial support (Project no. 10674090).

References

[1] J. Van Randeraat, R.E. Setterington, *Piezoelectric Ceramics*, Mullard Limited, London, 1974.
[2] W.P. Mason, *Physical Acoustics, vol. 1, Part A*, Academic Press, New York, London, 1964.
[3] O.E. Mattiat, *Ultrasonic Transducer Materials*, Plenum Press, New York, London, 1971.
[4] W.P. Mason, *Piezoelectric Crystals and Their Applications to Ultrasonics*, Van Nostrand, New York, 1950.
[5] R.D. Mindlin, Thickness–shear and flexural vibrations of crystal plate, *Journal of Applied Physics* 22 (1952) 316–323.
[6] C.V. Stephenson, Radial vibrations in short, hollow cylinders of barium titanate, *Journal of the Acoustical Society of America* 28 (1956) 51–56.
[7] G.E. Martin, Vibrations of longitudinally polarized ferroelectric cylindrical robes, *Journal of the Acoustical Society of America* 35 (1963) 510–520.
[8] A. Shoh, Sonic transducer, U.S. Patent No. 3,524,085, August 1970.
[9] E. A. Neppiras, The pre-stressed piezoelectric sandwich transducer, *Ultrasonics International 1973 Conference Proceedings*, Vol. 295.
[10] R.E. Horito, Free-flooding unidirectional resonators for deep-ocean transducers, *Journal of the Acoustical Society of America* 41 (1967) 158–166.
[11] S.Y. Lin, Design of piezoelectric sandwich ultrasonic transducers with large cross-section, *Applied Acoustics* 44 (1995) 249–257.
[12] S. Sherrity, H.D. Wiedericky, B.K. Mukherjeey, M. Sayerz, An accurate equivalent circuit for the unloaded piezoelectric vibrator in the thickness mode, *Journal of Physics D: Applied Physics* 30 (1997) 2354–2363.
[13] F.J. Arnold, S.S. Muhlen, The mechanical pre-stressing in ultrasonic piezotransducers, *Ultrasonics* 39 (2001) 7–11.
[14] G.P. Zhou, The performance and design of ultrasonic vibration system for flexural mode, *Ultrasonics* 38 (2000) 979–984.
[15] K.D. Rolt, History of the flextensional electroacoustic transducer, *Journal of the Acoustical Society of America* 87 (1990) 1340–1349.
[16] J.F. Tressler, R.E. Newnham, Capped ceramic underwater sound projector: the "cymbal" transducer, *Journal of the Acoustical Society of America* 105 (1999) 591–600.
[17] J.D. Zhang, W.J. Hughes, R.J. Meyer Jr., K.J. Uchino, R.E. Newnham, Cymbal array: a broad band sound projector, *Ultrasonics* 37 (2000) 523–529.
[18] C.L. Sun, S.S. Guo, W.P. Li, Z.B. Xing, G.C. Liu, X.Z. Zhao, Displacement amplification and resonance characteristics of the cymbal transducers, *Sensors and Actuators A* 121 (2005) 213–220.
[19] J.F. Tressler, R.E. Newnham, Doubly resonant cymbal-type transducers, *IEEE Transactions on Ultrasonics, Ferroelectrics, and Frequency Control* 44 (1997) 1175–1177.